Cancer Research

Tim-3 Expression on Tumor-Infiltrating PD-1$^+$CD8$^+$ T Cells Correlates with Poor Clinical Outcome in Renal Cell Carcinoma

Clémence Granier[1], Charles Dariane[1,2], Pierre Combe[1,3], Virginie Verkarre[4], Saïk Urien[5,6], Cécile Badoual[1,4], Hélène Roussel[1,4], Marion Mandavit[1], Patrice Ravel[7], Mathilde Sibony[8], Lucie Biard[9], Camélia Radulescu[10], Emeline Vinatier[1,11], Nadine Benhamouda[1,11], Michael Peyromaure[12], Stéphane Oudard[1,3], Arnaud Méjean[2], Marc-Olivier Timsit[2], Alain Gey[1,11], and Eric Tartour[1,11]

Abstract

Inhibitory receptors expressed by T cells mediate tolerance to tumor antigens, with coexpression of these receptors exacerbating this dysfunctional state. Using the VectraR automated multiparametric immunofluorescence technique, we quantified intratumoral CD8$^+$ T cells coexpressing the inhibitory receptors PD-1 and Tim-3 from patients with renal cell carcinoma (RCC). A second validation cohort measured the same parameters by cytometry. The percentage of tumor-infiltrating CD8$^+$ T cells coexpressing PD-1 and Tim-3 correlated with an aggressive phenotype and a larger tumor size at diagnosis. Coexpression of PD-1 and Tim-3 above the median conferred a higher risk of relapse and a poorer 36-month overall survival. Notably, other CD8$^+$T-cell subsets did not exert a similar effect on overall survival. Moreover, only the PD-1$^+$Tim-3$^+$ subset of CD8$^+$T cells exhibited impaired function after stimulation. Our findings establish intratumoral Tim-3$^+$PD1$^+$CD8$^+$ T cells as critical mediators of an aggressive phenotype in RCC. Use of the Vectra tool may be useful to identify similarly critical prognostic and predictive biomarkers in other tumor types and their response to immunotherapy. *Cancer Res; 77(5); 1075–82. ©2016 AACR.*

Introduction

Immunotherapy based on inhibition of checkpoint inhibitors (CTLA-4, PD-1) expressed on T cells has been demonstrated to be clinically effective in various phase III clinical trials in metastatic melanoma, non–small cell lung carcinoma (NSCLC), and renal cell carcinoma (RCC; ref. 1). Overall, this novel therapeutic approach achieves about 30% of clinical responses in cancer patients (2). Preexisting antitumor CD8$^+$ T cells appear to be required for the success of PD-1–PD-L1/2 blockade in cancer patients (3). Various arguments suggest that coexpression of inhibitory receptors (PD-1, CTLA-4, Tim-3, Lag3, etc.) on CD8$^+$ T cells may represent a clue to explain resistance mechanisms to checkpoint inhibitor blockade. Indeed coexpression of distinct inhibitory receptors has been associated with greater T-cell exhaustion and resistance to the ability of anti-PD-1/PD-L1 antibodies to restore these dysfunctional T cells in both infections and cancer (4–7).

Up until now, coexpression of inhibitory receptors has mainly been performed on fresh tumor cells by multiparametric cytometric analysis, which precludes determination of the prognostic significance of this parameter on large cohorts of patients or in retrospective studies. To overcome this drawback, we have developed multiparametric *in situ* immunofluorescence analysis with multispectral imaging.

In humans, RCC represents a good model to analyze the clinical significance of this coexpression, as previous studies have already detected inhibitory receptors (PD-1, Lag3, PD-L1, and PD-L2) associated with poor prognosis in this cancer (8, 9). We have focused on the expression of PD-1 and Tim-3 on CD8$^+$ T cells, as PD-1 and Tim-3 coexpression has been shown to be correlated with T-cell dysfunction in murine acute myelogenous leukemia, human melanoma, and NSCLC (4, 10, 11). VHL gene inactivation in most RCCs with clear cell histology results in the overexpression of VEGF, explaining why RCC is a highly vascular cancer. We have recently shown that VEGF induces PD-1 and Tim-3 expression on CD8$^+$ T cells (12). Finally, The Cancer Genome Atlas database has reported high Tim-3 expression in clear cell RCC (ccRCC; ref. 13), but as Tim-3 can also be expressed by many cells, including tumor,

[1]INSERM U970, Université Paris Descartes, Sorbonne Paris-Cité, Paris, France. [2]Department of Urology, Hôpital Européen Georges Pompidou, Paris, France. [3]Service d'Oncologie Médicale, Hôpital Européen Georges Pompidou, Paris, France. [4]Department of Pathology, Hôpital Européen Georges Pompidou, Paris, France. [5]EA08: Evaluation des Thérapeutiques et Pharmacologie Périnatale et Pédiatrique, Unité de Recherche Clinique Paris Centre, Paris, France. [6]CIC 1419 INSERM Cochin-Necker, Paris, France. [7]CNRS UMR5048 Centre de Biochimie Structurale, INSERM U554, Université de Montpellier 1 et 2, Montpellier, France. [8]Department of Pathology, Hôpital Cochin, Paris, France. [9]Université Paris Diderot Paris 7, Paris, France. [10]Department of Pathology, Hôpital Foch, Suresnes, France. [11]Service d'Immunologie Biologique, AP-HP, Hôpital Européen Georges Pompidou, Paris, France. [12]Department of Urology, Hôpital Cochin, Paris, France.

Note: Supplementary data for this article are available at Cancer Research Online (http://cancerres.aacrjournals.org/).

C. Granier and C. Dariane contributed equally to this article.

A. Gey and E. Tartour are the principal investigators of this article.

Corresponding Author: Eric Tartour Hôpital Européen Georges Pompidou. Service d'Immunologie Biologique. 20 Rue Leblanc 75015 Paris. Phone: 33156093942; Fax: 33156092080; E-mail: eric.tartour@aphp.fr

doi: 10.1158/0008-5472.CAN-16-0274

myeloid, and endothelial cells, only multiparametric *in situ* immunofluorescence analysis will allow accurate definition of its role and clinical significance when expressed on $CD8^+$ T cells. The aim of this study was to evaluate the biological significance and clinical impact of Tim-3 coexpression on PD-1^+ tumor-infiltrating $CD8^+$ T cells in RCC patients.

Materials and Methods

Patient cohorts

Two independent cohorts of nontreated RCC patients who underwent partial or radical nephrectomy in the Urology Department of European Georges Pompidou or Necker or Cochin Hospitals (Paris, France) were included in this study. One cohort was a retrospective cohort of 87 nonmetastatic ccRCC patients who underwent surgery between April 1999 and June 2005 and who were selected from the Necker Hospital biobank for multiparametric *in situ* immunofluorescence analysis.

A second independent prospective cohort included 42 patients enrolled between February 2012 and November 2015 at European Georges Pompidou or Cochin Hospitals. All histologic cancer types were included in this cohort except for cystic lesions.

Patient characteristics of the two cohorts are reported in Supplementary Tables S1 and S2. This study was conducted in accordance with the Declaration of Helsinki and was approved by the local ethics committee (CPP Ile de France nr. 2012-05-04). Informed consent was obtained from all participants.

Immunophenotyping by cytometry analysis

Immunofluorescence staining and flow cytometry analysis of tumor-infiltrating lymphocytes (TIL) are performed as described previously (14) Briefly, after dissociation of nephrectomy piece by DNAse I (30 IU/mL, Roche) and collagenase D (1 mg/mL, Roche) for 60 minutes, cells were stained with a fixable viability stain FVS 520 (eBioscience), BV510-labeled anti-CD3 (BD Biosciences), PE-labeled anti-CD8 (BD Biosciences), BV421-labeled anti-PD-1 (BD Biosciences) and APC-labeled anti-Tim-3 (BioLegend/Ozyme). For the analysis, cells were gated on viable singlet positive $CD3^+$ T cells. Isotype control antibodies were included in each experiment.

A detailed description of the used antibodies is presented in Supplementary Table S3.

In situ immunofluorescence staining of TILs

Tissue samples obtained on the day of surgery were frozen and stored at −80°C. The quality of the sample was checked on an H&E-stained section examined by a pathologist. Frozen specimens were sectioned at 4 to 6 μm with a cryostat, placed on slides, air dried, and fixed for 5 minutes with 100% acetone. Before incubation with antibodies, the slides were pretreated with avidin/biotin blocker (DAKO) for 10 minutes, and Fc receptors were blocked with 5% donkey serum (DAKO) in TBS for 30 minutes. Staining for CD8, PD-1, Tim-3, PD-L1, galectin-9, and Pax8 was performed using nonlabeled primary antibodies followed by fluorophore-labeled secondary antibodies. Pan-keratin was stained with an AF647-labeled antibody. These antibodies are described in Supplementary Table S3. Isotype-matched antibodies were used as negative controls. In each case, we checked that secondary antibodies did not crossreact with unrelated primary antibodies used in the combination. Nuclei were highlighted using DAPI mounting medium.

Fluorescence analysis and automated cell count

Slides of stained renal sections were read with an automated Vectra microscope. This PerkinElmer technology can be used to measure thermophometric and fluorescence characteristics in the various cell compartments (membrane/cytoplasm/nuclei). A coupled inForm software integrates these various signals, allowing a multiplex staining protocol. As recommended for multiplex analysis, single-stained (Cyanine 5 or Cyanine 3 or Alexa Fluor 488 or AF647 or FITC depending on the staining) and nonstained slides were analyzed in inForm to integrate the corresponding spectra in a fluorescence library. For each slide, image acquisition and subsequent counts were performed on at least 5 fields. inForm software allows cell segmentation and phenotyping. Briefly, for cell recognition, "cell segmentation" was based on DAPI staining and cell size. Then, a phenotyping step, which was based on the teaching of the software for positive and negative cells, was performed to define an algorithm program of analysis (refer to Fig. 1). Cells monostained for CD8 (blue dot) or costained for PD-1 and CD8 (red dot) or PD-1, Tim-3, and CD8 (green dot) were manually identified until the automatized recognition by the inForm software was concordant with visual count (error < 5%). The counting of CD3 and the percentage of expression of PD-L1, Tim-3, and galectin-9 on tumor cells was also performed on the Inform software after the analysis with the vectra microscope.

The mean of positive-stained cells in at least five fields using a 20× objective was selected for each analysis. For the phenotyping step, an independent operator and a pathologist confirmed the visual inspection. Each phenotyping image was checked after software analysis. The use of software to compute the pure spectrum of a fluorophore from a mixed emission signal, combined with automated image analysis, avoids the usual risk of overlapping signals from various fluorophores and interoperator variability of manual counting.

Cell sorting and T-cell activation

Fresh TILs obtained after DNase/collagenase digestion were stained with anti-CD3, anti-CD8, anti-PD-1, and anti-Tim-3 and were sorted into three populations PD-1^+Tim-$3^+$$CD8^+$, PD-$1^+$Tim-$3^-$$CD8^+$, and PD-$1^-$Tim-$3^-$$CD8^+$ using a FACSARIA sorter (BD Biosciences). Recovered T cells were incubated for 24 hours with medium or stimulated with an anti-CD3–anti-CD28 T Cell Activation Kit (Miltenyi Biotec). IFNγ was measured by ELISA (Diaclone) in the supernatants collected before or 24 hours after T-cell activation. In independent experiments, bulk TILs were activated by anti-CD3 and anti-CD28 in the presence of neutralizing anti-PD-1 [monoclonal human IgG4 (S228P), Invivogen] and anti-Tim-3 [monoclonal IgG1 (F38-2E2), eBioscience] antibodies.

Statistical analysis

Statistical analyses were performed with R software and the survival package (15). Results were compared by a χ^2 test or Wilcoxon rank tests, as appropriate. Covariate(s) effect(s) on survival was analyzed using the Cox model. Probit regression model was also used to fit the relationship between patient status (dead or still alive) and the variable. Progression-free survival (PFS) was estimated using the Kaplan–Meier method. All tests were two-sided and *P* values lower than 0.05 were considered as significant.

Results

Detection and characterization of CD8$^+$ T cells with or without PD-1 and Tim-3 coexpression by automated *in situ* immunofluorescence spectral imaging

To characterize RCC-infiltrating CD8$^+$ T cells expressing PD-1 and Tim-3, we set up a multifluorescence *in situ* technique with automated counting (Fig. 1). We showed that about one half of CD8$^+$ T cells express PD-1 (mean, 53.9%; SE, 30.49%; Supplementary Fig. S1A). This population can be divided into two groups: (i) one corresponding to double positive PD-1$^+$Tim-3$^+$ CD8$^+$ T cells with a mean percentage of 38.16% (SE, 28.11%); (ii) a second population of CD8$^+$ T cells expressing PD-1 without Tim-3 (mean, 15.77%; SE, 8.62%; Supplementary Fig. S1A). It is noteworthy that Tim-3 expression without PD-1 expression was detected in less than 3% of CD8$^+$ T cells (data not shown). The mean numbers of total CD8$^+$ T cells, PD-1$^+$ CD8$^+$T cells, PD-1$^+$Tim-3$^+$, and PD-1$^+$Tim-3$^-$ CD8$^+$ T cells were 116.5 (SE, 216), 89.32 (SE, 191.8), 66.9 (SE, 143), and 22.38 (SE, 57.5), respectively (Supplementary Fig. S1B). As expected, Tim-3 expression was also observed on non-CD8$^+$ T cells and non-CD3$^+$ T cells (Fig. 1 and Supplementary Fig. S7C). A correlation was found between the total number of intratumor CD8$^+$ T cells and the percentage of PD-1$^+$ Tim-3$^+$ on CD8$^+$ T cells (Supplementary Fig. S1C).

Clinical significance of PD-1 and Tim-3 coexpression on CD8$^+$ T cells by *in situ* fluorescence analysis

Various criteria [tumor–node–metastasis (TNM), Fuhrman grade, tumor size, and UCLA Integrated Staging System (UISS) score] have been proposed to define the prognosis value of primary RCC. The percentage or number of tumor-infiltrating CD8$^+$ T cells expressing PD-1 without Tim-3 was not correlated with any of the above criteria of aggressiveness (Table 1 and Supplementary Table S4). In contrast, a positive correlation was observed between the percentage of tumor-infiltrating CD8$^+$ T cells expressing PD-1 (i.e., Tim-3$^+$ or Tim-3$^-$) or coexpressing PD-1 and Tim-3 and TNM stage, Fuhrman grade, and UISS score (Table 1 and Supplementary Fig. S2). PD-1 and Tim-3 coexpression was also associated with larger tumor size (Supplementary Fig. S2). The number of

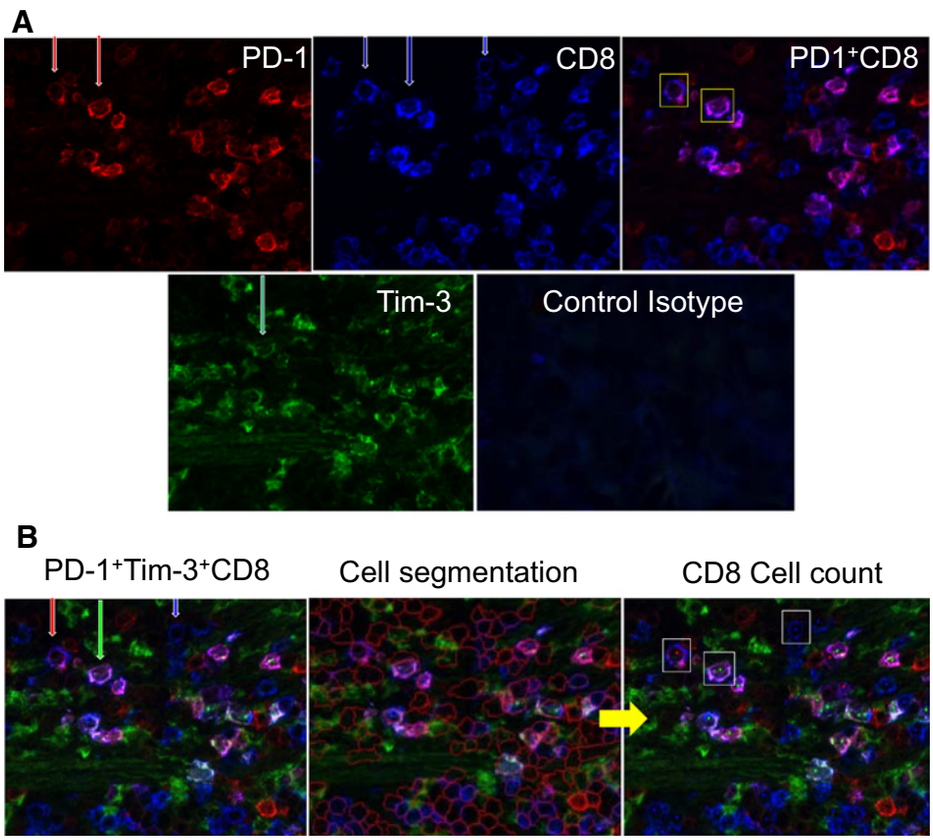

Figure 1.
PD-1 and Tim-3 expression on tumor-infiltrating CD8$^+$ T cells from a patient with ccRCC. **A,** Frozen tissue sections derived from RCC patients were stained by immunofluorescence with antibodies directed against human PD-1, CD8, and Tim-3. Colored arrows, cells expressing CD8 (blue), PD-1 (red), and Tim-3 (green). Colocalization of these three markers can be detected by merging the monostaining picture. Yellow boxes, cells expressing both CD8 and PD-1. Staining with isotype controls was included for each experiment. **B,** Triple costaining for CD8, PD-1, and Tim-3 (merged) is shown on the left, with the green arrow indicating CD8$^+$ T cells coexpressing PD-1 and Tim-3, the red arrow corresponding to CD8$^+$ T cells expressing PD-1, and the blue arrow identifying CD8$^+$ T cells not expressing PD-1 or Tim-3. For automated counting, inForm software allows cell segmentation based on DAPI staining of the nucleus and morphometric characteristics (middle). An automated count based on a user-defined algorithm was then performed (right), which generated green dots corresponding to CD8$^+$ T cells coexpressing PD-1 and Tim-3, red dots corresponding to CD8$^+$ T cells expressing PD-1 without Tim-3, and blue dots corresponding to CD8$^+$ T cells not expressing PD-1 or Tim-3. (original magnification, ×200).

Table 1. Correlation between the expression of PD-1 alone or combined with Tim-3 on $CD8^+$ T cells and clinical prognostic parameters of RCC patients

	$PD\text{-}1^+$		$PD1^+Tim\text{-}3^+$		$PD\text{-}1^+Tim\text{-}3^-$	
%/CD8	IF	Cytm	IF	Cytm	IF	Cytm
TNM	**0.04**	0.28	**0.003**	**0.047**	0.22	0.77
Fuhrman	**0.01**	0.25	**0.004**	0.58	0.74	0.33
Tumor size	0.08	0.22	**0.01**	**0.02**	0.37	0.39
UISS	**0.01**	**0.01**	**0.01**	**0.049**	0.63	0.2

NOTE: The percentage of $PD\text{-}1^+$, $PD\text{-}1^+Tim\text{-}3^+$, or $PD\text{-}1^+Tim\text{-}3^-$ on $CD8^+$ T cells selected as a continuous variable measured by either *in situ* immunofluorescence (IF) in the first cohort of patients ($n = 87$) or cytometry (Cytm) in the second cohort of patients ($n = 42$) was correlated with various clinical parameters defined as a binary (TNM, Fuhrman grade, and UISS score) or a continuous variable (tumor size). TNM was divided into two groups: localized disease (pT1 and pT2) and advanced disease (pT3, pT4, N^+, or M^+). Fuhrman grade was defined as low (grade I or II) and high (grade III or IV), and the UISS score was divided into three classes (0, 1, and 2). *P* values indicating a significant correlation are shown in bold.

tumor-infiltrating $CD8^+$ T cells expressing PD-1 or coexpressing PD-1 and Tim-3 was also correlated with Fuhrman grade and UISS score (Supplementary Table S4). In line with this more pejorative phenotype, RCC patients with $CD8^+$ T cells coexpressing PD-1 and Tim-3 above the median (34.7) were more likely to relapse [$P = 0.046$; HR, 2.9; 95% confidence interval (CI), 1.02–8.21; Fig. 2B]. This correlation was not observed with the percentage of PD-1 on $CD8^+$ T cells (Fig. 2A). A correlation was also demonstrated between the percentage of $CD8^+$ T cells coexpressing PD-1 and Tim-3 and the 36-month overall survival (OS) rate (Fig. 2B). This same group of patients also presented a trend toward poorer OS when the median was selected as cutoff ($P = 0.079$; HR, 2.16; 95% CI, 0.91–5.1). When the total number of $CD3^+$ T cells, $CD8^+$ T cells, or all other CD8 subsets was analyzed as a continuous variable or binary variable defined by the median, even if a trend remains toward more relapse for the patients with $CD8^+$ T cells coexpressing PD-1 and Tim-3 above the median ($P = 0.0859$), no significant statistical correlation was observed with PFS or OS (Supplementary Fig. S3 and data not shown). Only the percentage of PD-1 and Tim-3 coexpression on $CD8^+$ T cells had an impact on the patients' clinical outcome.

Assessment of PD-1 and Tim-3 coexpression on $CD8^+$ T cells by cytometry and its clinical significance

To validate these results, we measured PD-1 and Tim-3 expression on $CD8^+$ T cells by cytometry in a series of 42 fresh tumors derived from RCC patients (Supplementary Fig. S4). As previously observed with the multiparametric immunofluorescence *in situ* technique, about one half of $CD8^+$ T cells expressed PD-1 (mean 50.8 ± 20.76), and no $CD8^+$ T cells expressed Tim-3 without PD-1. In the overall population, 15% of $CD8^+$ T cells coexpressed PD-1 and Tim-3, and this percentage increased to 17.42% in the more restricted group of ccRCC patients (Supplementary Fig. S5). Although the two series of patients were independent, we were surprised to find that the percentage of PD-1 expression on $CD8^+$ T cells was concordant with the two techniques, in contrast with Tim-3 expression. We confirmed that this difference was not due to the independent series of patients tested. As shown in Supplementary Fig. S6A, in the same group of 35 RCC patients for whom both TIL and frozen sections were available, the percentage of $PD\text{-}1^+Tim\text{-}3^+$ $CD8^+$ T cells was higher when detected by *in situ* immunofluorescence technique than by cytometry after collagenase dissociation ($P = 0.003$). In contrast, the percentage of $PD\text{-}1^+$ on $CD8^+$ T cells was similar when detected by *in situ* immunofluorescence technique and cytometry after collagenase dissociation, explaining the concordant results obtained for this marker with these two techniques. Nonenzymatic dissociation of TIL did not lead to a decrease of the percentage of Tim-3 expression measured by cytometry analysis when compared with *in situ* immunofluorescence technique (Supplementary Fig. S6B). This discordance of Tim-3 expression after the use of collagenase was

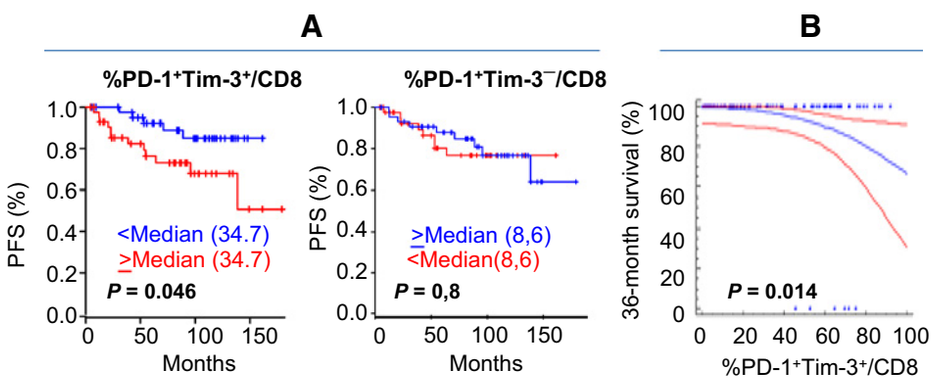

Figure 2.

Correlation between PD-1 and Tim-3 coexpression on $CD8^+$ T cells and clinical outcome. **A,** RCC patients ($n = 87$) were divided into two groups depending on whether the percentage of PD-1 without Tim-3 coexpression (right), PD-1 and Tim-3 coexpression (left) on $CD8^+$ T cells was above or below the median (34.7). Kaplan–Meier curves for PFS for the two groups of patients are shown. **B,** The correlation between the percentage of PD-1 and Tim-3 coexpression on $CD8^+$ T cells selected as a quantitative variable and the 36-month OS is shown (probit regression model). The blue line corresponds to this correlation, whereas the red line represents the upper or lower limits of the 95% CI. Blue squares on the top indicate that the corresponding patients are alive, whereas blue squares on the bottom correspond to deceased patients.

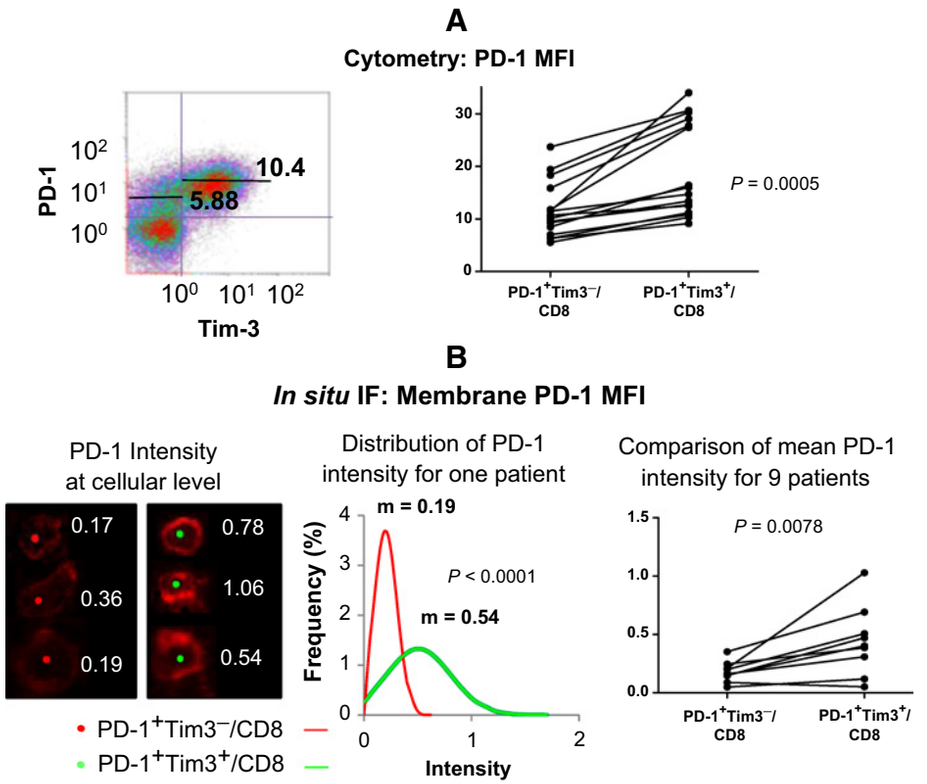

Figure 3.
PD-1$^+$Tim-3$^+$ coexpression on CD8$^+$ T cells correlates with high levels of PD-1. **A,** MFI of PD-1 measured by cytometry on PD-1$^+$Tim-3$^+$ and PD-1$^+$Tim-3$^-$ cells gated on CD8$^+$ T cells for one representative RCC patient (left).The result of the same analysis is shown (right) for 16 patients selected on the basis of PD-1 and Tim-3 coexpression by at least 10% of the total CD8$^+$ T-cell population (Wilcoxon test). **B,** Example of the intensity of PD-1 detected at the cellular level (left) by *in situ* immunofluorescence (IF) analysis on PD-1$^+$Tim-3$^+$ and PD-1$^+$Tim-3$^-$ CD8$^+$ T cells and at the individual level (middle); example from the third cell at the bottom of the left panel (middle) after integrating the various cell signals on a tissue section (Mann–Whitney test). Comparative analysis of the mean PD-1 intensity measured by *in situ* immunofluorescence on the two CD8$^+$ T-cell subsets (PD-1$^+$Tim-3$^-$ and PD-1$^+$Tim-3$^+$) in a series of 9 patients (right) for whom both tissue sections and TILs were available (Wilcoxon test).

further investigated by showing that TILs treated by collagenase presented decreased Tim-3 expression compared with TILs treated by a mechanical method of dissociation ($P = 0.028$; Supplementary Fig. S6C). Tim-3 expression on activated PBMCs was also decreased when these cells were treated by collagenase compared with mechanical dissociation in the absence of collagenase ($P = 0.029$; Supplementary Fig. S6D). Interestingly, collagenase did not affect the PD-1 expression of CD8$^+$ T cells, explaining the concordant results obtained for this marker with these two techniques. These results support the clinical value of a multiparametric *in situ* immunofluorescence technique to avoid this type of bias.

Regarding the clinical significance of cytometry results, we confirmed that the percentage of CD8$^+$ T cells expressing PD-1 without Tim-3 by cytometry analysis did not correlate with any of the prognostic criteria (TNM, Fuhrman grade, tumor size, and UISS score), whereas patients whose CD8$^+$ T cells coexpressed PD-1 and Tim-3 had a more advanced TNM stage ($P = 0.021$), larger tumor size ($P = 0.021$), and a higher UISS score ($P = 0.049$). Interestingly, Tim-3 and PD-1 coexpression on CD8$^+$ T cells was more intense in the group of patients with ccRCC, which is considered to be a more aggressive cancer than the chromophobe or tubulopapillary or oncocytoma subgroups (Supplementary Fig. S5). The follow-up of this prospective group of patients monitored by cytometry analysis was not sufficient to assess PFS and OS.

Apart from the absolute percentage of PD-1 and Tim-3 coexpression on CD8$^+$ T cells, all other parameters measured and their clinical significance were therefore very similar between the two series. All the raw data of the coexpression of PD-1 and Tim-3 from the two cohorts are shown in Supplementary Tables S5 and S6

Phenotypic and functional characterization of the population of CD8$^+$ T cells coexpressing PD-1 and Tim-3

As the levels of PD-1 expression on T cells have been shown to be correlated with T-cell exhaustion, defined by the expression of multiple inhibitory receptors (16), we determined PD-1 levels on CD8$^+$ T cells with or without Tim-3 coexpression. In the patient shown in Fig. 3A (left), we observed an increased expression of the mean fluorescence intensity (MFI) of PD-1, when it was coexpressed with Tim-3 (MFI, 10.4) compared with PD-1 expression alone (5.88). In a series of 16 patients, the MFI of PD-1 on CD8$^+$ T cells coexpressing Tim-3 (mean 19.13 ± 8.8) was also higher than the MFI observed on CD8$^+$ T cells not expressing Tim-3 (mean 11.58 ± 5.2; $P = 0.0063$; Fig. 3A, right). *In situ* immunofluorescence results are illustrated in Fig. 3B. An example of cell membrane PD-1 fluorescence intensity in one patient is shown (left), and the integration of more than 50 cells for this patient is represented (middle). In a series of 10 patients in the absence of Tim-3, the mean PD-1 fluorescence intensity was increased when PD-1 was coexpressed with Tim-3 (0.44 ± 0.29 vs. 0.18 ± 0.09, $P = 0.0123$; Fig. 3B, right). Thus, by using two different techniques, we demonstrated that PD-1 and Tim-3 coexpression was associated with higher levels of PD-1 expression on CD8$^+$ T cells.

To determine the putative difference in terms of functionality between PD-1$^+$Tim-3$^+$ CD8$^+$ T cells and PD-1$^+$Tim-3$^-$ CD8$^+$ T cells, we selected two patients with PD-1 and Tim-3 coexpression and sorted the following three populations: PD-1$^-$Tim-3$^-$CD8$^+$T cells, PD-1$^+$Tim-3$^-$CD8$^+$ T cells, and PD-1$^+$Tim-3$^+$CD8$^+$ T cells (Fig. 4, left). After stimulation with anti-CD3 and anti-CD28 mAb, we showed that the PD-1$^-$Tim-3$^-$ and PD-1$^+$Tim-3$^-$ populations secreted large quantities of IFNγ in their supernatants with no significant difference between the two subpopulations. In

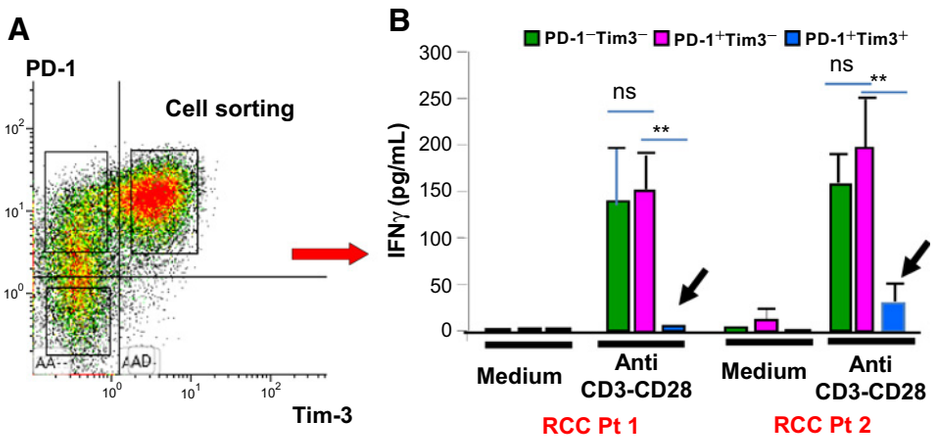

Figure 4.
Functional analysis of CD8$^+$ T cells depending on their expression of PD-1 alone or combined with Tim-3. **A**, CD8$^+$CD3$^+$ T cells were sorted on the basis of their PD-1 and Tim-3 expression into three cell populations: PD-1$^+$Tim-3$^+$, PD-1$^+$Tim-3$^-$, and PD-1$^-$Tim-3$^-$. **B,** Cells collected after sorting (10^5/well) were activated or not by anti-CD3 and anti-CD28 (2.5 millions beads per five 10^6 cells) for 24 hours, and IFNγ was then measured by ELISA in the supernatant. **, $P < 0.01$ (Wilcoxon test). ns, not significant.

contrast, IFNγ production was significantly decreased in CD8$^+$ T cells coexpressing PD-1 and Tim-3 compared with the other two populations (Fig. 4, right).

The addition of anti-PD-1 and anti-Tim-3 mAb on bulk TILs coexpressing PD-1 and Tim-3 increased the production of IFNγ in 2 of 3 TILs tested (Supplementary Fig. S8).

Expression of the ligands of PD-1 and Tim-3 on renal tumor cells

As T-cell exhaustion is mediated through receptor/ligand interaction, to support the *in vivo* relevance of the expression of PD-1 and Tim-3 in the subpopulations of CD8$^+$T cells, we checked for the expression of their main ligands, PD-L1 and galectin-9, on renal tumor cells. We found that with a cut-off of 10% of positive tumor cells, 58 out of 87 patients (66%) were positive for the expression of PD-L1. Of note, PD-L1 could also be expressed on nontumor cells (Fig. 5A). A double immunostaining with an anti-pan-keratin and an anti-galectin-9 antibodies showed that with a cut-off of 10% of positive tumor cells, all the tumors analyzed were positive for Gal-9 (Fig. 5B). Interestingly, PD-1 was not expressed by tumor cells (Supplementary Fig. 7A), while with a cut-off of 10% of positive cells, 12.1% of tumors were positive for Tim-3 (Supplementary Fig. 7B). Tim-3 could also be expressed on cells other than tumor cells or T cells (Supplementary Fig. 7C).

Discussion

Using a novel multiparametric *in situ* immunofluorescence spectral imaging technology, we showed that the clinical significance of PD-1 expression by CD8$^+$ T cells differed according to whether or not PD-1 was coexpressed with Tim-3. Indeed, we showed that RCC patients with tumor-infiltrating CD8 cells that coexpressed PD-1 and Tim-3 presented a more aggressive phenotype defined by high Fuhrman grade and larger tumor size and more advanced TNM and UISS scores. This group of patients also exhibited decreased PFS and 36-month OS. This aggressive phenotype was confirmed by cytometry analysis, as patients whose CD8$^+$ T cells coexpressed PD-1 and Tim-3 had more advanced TNM stage and UISS score and larger tumor size.

These data may explain some of the controversies in the literature concerning the prognostic value of PD-1 (8, 14, 17–19) and emphasize the critical role of combined expression of coinhibitory receptors, especially Tim-3, in the clinical significance of PD-1. This complex interpretation of the clinical value of PD-1 is consistent with its multiple biological roles, as PD-1 is both an activation marker and a hallmark of exhausted T cells. However, PD-1 also protects CD8$^+$T cells from overstimulation and the risk of accumulation of terminally differentiated exhausted CD8$^+$ T

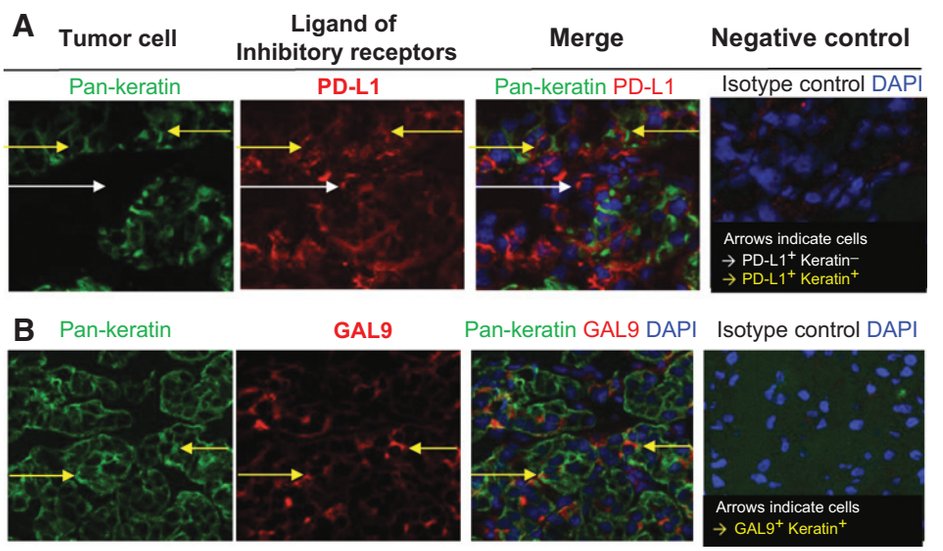

Figure 5.
Expression of PD-1 ligand and galectin-9 on renal cell carcinoma. Frozen tissue sections derived from RCC patients were stained by immunofluorescence with antibodies directed against PD-L1 (**A**), galectin-9 (GAL9; **B**) and pan-keratin (**A** and **B**). Colocalization of these markers can be detected by merging the monostaining picture. Dapi staining and isotype controls were included for each staining. White arrow, PD-L1$^+$ pan-keratin$^+$ cells (**A**); yellow arrow, PD-L1$^+$ pan-keratin$^+$ cells (**A**) or galectin+pan-keratin$^+$ cells (**B**). Original magnification, ×200.

cells (20). Although Tim-3 is also induced after activation (20), its coexpression with PD-1 in the tumor microenvironment may represent a switch, leading to compromised T-cell function (4, 21, 22). We showed that the CD8$^+$ T-cell population coexpressing PD-1 and Tim-3 presented all of the features of an exhausted T-cell population, as they responded poorly to T-cell stimulation. In addition, high levels of PD-1 expressed at the CD8$^+$ T-cell membrane are considered to be a hallmark of particularly dysfunctional T cells (11, 16). Interestingly, both *in vitro* and *in vivo*, Tim-3–Tim-3 ligand blockade in combination with inhibition of the PD-1–PD-L1 pathway synergized to restore T-cell function, resulting in the control of chronic infection and inhibition of tumor growth (4, 5, 23–25). In addition to activation, Th1 cytokines may also promote PD-1 and Tim-3 coexpression, as type I and II IFN–regulated PD-1 and IL12 and IL27 enhanced Tim-3 expression (21, 26, 27). Tumor-associated M2 macrophages also regulated Tim-3 expression on T cells derived from RCC (28). We recently showed that VEGF also enhanced the expression of PD-1 and Tim-3 after activation (12).

Coexpression of PD-1 and Tim-3 could also be detected on T cells other than CD8$^+$ T cells such as regulatory T cells. In our series of patients, with a positive threshold of 10%, 47.3% of Treg from RCC patients coexpressed PD-1 and Tim-3.

Tim-3 may also be expressed on non–T cells, such as myeloid cells conferring impaired immunosurveillance to these cells (29, 30). In RCC, Tim-3 has been shown to be expressed in macrophages and tumor cells (31). We confirmed that 12.1% of RCC tumors could express Tim-3 (Supplementary Fig S7). Tim-3 promoted ccRCC invasion and made these cells more resistant to antiangiogenic molecules (31). In addition, in the tumor microenvironment, Tim-3 has been detected in the majority of regulatory T cells (Treg), and these Tregs coexpressing PD-1 were highly suppressive (32).

Tim-3$^+$ tumor-infiltrating CD8$^+$ T cells have been correlated with histologic grade and advanced tumor stage in follicular lymphoma and NSCLC, respectively, but no data are available concerning their influence on clinical outcome (11, 21). Furthermore, higher Tim-3 gene expression in RCC has been shown to be a marker for poorer 5-year survival (13). In contrast with cancer, Tim-3$^+$CD8$^+$ T cells may have a less pejorative significance in preneoplastic lesions, such as usual-type vulvar intraepithelial neoplasia, as it has been correlated with an absence of recurrence. However, greater numbers of Tim-3$^+$ CD8$^+$ T cells were observed in vulvar carcinoma compared with benign lesions (33).

All these data converge to target Tim-3 in cancer alone or preferably in combination with anti-PD-1/PD-L1.

Other checkpoint inhibitors, such as Lag-3, may also be coexpressed with PD-1 on CD8$^+$ T cells, as observed in RCC and other tumors, and it is usually correlated with impaired effector function of these cells (9, 34). Interestingly, in NSCLC, CD8$^+$ T cells expressing Tim-3 are those that coexpressed the greatest number of other inhibitory receptors compared with cells expressing other checkpoint inhibitors, possibly making Tim-3 a surrogate marker for more advanced exhausted T cells (11).

One limitation of this study is that the CD8$^+$ T-cell population was not compartmentalized in the tumor core or stroma due to difficulties of combining a homogeneous tumor cell marker with our set of T-cell antibodies. As the prognostic value of T-cell subpopulations has been shown to depend on their location in the tumor core or in the periphery, this could explain certain minor discrepancies between our results and those reported in the literature concerning the prognosis value of the numbers of CD8$^+$ T cells and PD-1$^+$ T cells (8, 9, 35). The site of T cells could also explain the more significant impact of the percentage expression of inhibitory receptors, PD-1 and Tim-3, over the number of cells expressing these markers, as this percentage reflects an intrinsic aspect of the exhausted status of tumor-infiltrating CD8$^+$ T cells. The influence of the number of PD-1$^+$Tim-3$^+$ CD8$^+$ T cells may be more dependent on their ratio with respect to the number of tumor cells. In addition, most published studies used a monoparametric immunochemistry technique for the analysis of checkpoint inhibitor expression, in contrast with our focus on characterization of checkpoint inhibitors specifically on CD8$^+$ T cells considered to be one of the main effectors after immunotherapy (3). The various variables were also defined either as a continuous variable or with a median cutoff in our current study, which differs from previous studies that used optimal *P* values (8, 9).

We have shown that collagenase may decrease the expression of some parameters, such as Tim-3, when detected by cytometry, which reinforces the value of our automated multiparametric *in situ* immunofluorescence technique to directly assess *in vivo* intratumor expression of checkpoint inhibitors in untouched cells. This novel technology used in this study and recently described by other groups (3, 36) will allow more accurate characterization of CD8$^+$ T cells and other immune cells at the single-cell level in the tumor microenvironment, allowing more precise guidance of the choice of immune target for immunotherapy.

In addition, the fact that, in contrast with the PD-1$^+$Tim-3$^-$CD8$^+$ T-cell population, double-positive PD-1$^+$Tim-3$^+$CD8$^+$ T cells could not be activated *in vitro* by a strong stimulus suggests that it may also be difficult to reactivate these cells after PD-1-PD-L1 blockade and that this double labeling could constitute a biomarker of resistance to immunotherapy.

Disclosure of Potential Conflicts of Interest

No potential conflicts of interest were disclosed.

Authors' Contributions

Conception and design: C. Granier, P. Combe, M. Mandavit, A. Méjean, M.-O. Timsit, A. Gey, E. Tartour

Development of methodology: C. Granier, P. Combe, H. Roussel, M. Mandavit, L. Biard, A. Gey, E. Tartour

Acquisition of data (provided animals, acquired and managed patients, provided facilities, etc.): C. Granier, C. Dariane, P. Combe, V. Verkarre, H. Roussel, M. Sibony, C. Radulescu, E. Vinatier, M. Peyromaure, M.-O. Timsit, A. Gey, E. Tartour

Analysis and interpretation of data (e.g., statistical analysis, biostatistics, computational analysis): C. Granier, C. Dariane, P. Combe, S. Urien, C. Badoual, P. Ravel, L. Biard, M. Peyromaure, S. Oudard, A. Méjean, A. Gey, E. Tartour

Writing, review, and/or revision of the manuscript: C. Granier, C. Dariane, P. Combe, S. Urien, S. Oudard, A. Méjean, M.-O. Timsit, A. Gey, E. Tartour

Administrative, technical, or material support (i.e., reporting or organizing data, constructing databases): C. Granier, C. Dariane, C. Badoual, H. Roussel, N. Benhamouda, M.-O. Timsit

Study supervision: M.-O. Timsit, A. Gey, E. Tartour

Acknowledgments

We thank the staff of the tumor banks of Necker, Foch, and European Georges Pompidou Hospitals as well as Urology Department of HEGP (Cedric Lebacle) for providing the sample materials and the Histology platform of PARCC European Georges Pompidou Hospital.

Grant Support

This work was supported by Labex Immuno-oncology (E. Tartour), Site Intégré de Recherche en Cancérologie (SIRIC CARPEM: fellowship to C. Granier), Cancérologie du Centre (CANCEN: fellowship to P. Combe), Université

Paris Sorbonne cite (grant Idex BioSPc to E. Tartour), ANR (Agence Nationale Recherche: project Selectimmunonco to E. Tartour), Ligue contre le Cancer (Equipe Labellisée; to E. Tartour), and INCa (AAPPLBio; to E. Tartour).

The costs of publication of this article were defrayed in part by the payment of page charges. This article must therefore be hereby marked *advertisement* in accordance with 18 U.S.C. Section 1734 solely to indicate this fact.

Received February 2, 2016; revised October 8, 2016; accepted October 29, 2016; published OnlineFirst November 21, 2016.

References

1. Lipson EJ, Forde PM, Hammers HJ, Emens LA, Taube JM, Topalian SL. Antagonists of PD-1 and PD-L1 in cancer treatment. Semin Oncol 2015;42:587–600.
2. Sharma P, Allison JP. The future of immune checkpoint therapy. Science 2015;348:56–61.
3. Tumeh PC, Harview CL, Yearley JH, Shintaku IP, Taylor EJ, Robert L, et al. PD-1 blockade induces responses by inhibiting adaptive immune resistance. Nature 2014;515:568–71.
4. Fourcade J, Sun Z, Benallaoua M, Guillaume P, Luescher IF, Sander C, et al. Upregulation of Tim-3 and PD-1 expression is associated with tumor antigen-specific CD8+ T cell dysfunction in melanoma patients. J Exp Med 2010;207:2175–86.
5. Sakuishi K, Apetoh L, Sullivan JM, Blazar BR, Kuchroo VK, Anderson AC. Targeting Tim-3 and PD-1 pathways to reverse T cell exhaustion and restore anti-tumor immunity. J Exp Med 2010;207:2187–94.
6. Baitsch L, Fuertes-Marraco SA, Legat A, Meyer C, Speiser DE. The three main stumbling blocks for anticancer T cells. Trends Immunol 2012;33:364–72.
7. Wherry EJ, Kurachi M. Molecular and cellular insights into T cell exhaustion. Nat Rev Immunol 2015;15:486–99.
8. Thompson RH, Dong H, Kwon ED. Implications of B7-H1 expression in clear cell carcinoma of the kidney for prognostication and therapy. Clin Cancer Res 2007;13:709s–715s.
9. Giraldo NA, Becht E, Pages F, Skliris G, Verkarre V, Vano Y, et al. Orchestration and prognostic significance of immune checkpoints in the microenvironment of primary and metastatic renal cell cancer. Clin Cancer Res 2015;21:3031–40.
10. Zhou Q, Munger ME, Veenstra RG, Weigel BJ, Hirashima M, Munn DH, et al. Coexpression of Tim-3 and PD-1 identifies a CD8+ T-cell exhaustion phenotype in mice with disseminated acute myelogenous leukemia. Blood 2011;117:4501–10.
11. Thommen DS, Schreiner J, Muller P, Herzig P, Roller A, Belousov A, et al. Progression of lung cancer is associated with increased dysfunction of T cells defined by coexpression of multiple inhibitory receptors. Cancer Immunol Res 2015;3:1344–55.
12. Voron T, Colussi O, Marcheteau E, Pernot S, Nizard M, Pointet AL, et al. VEGF-A modulates expression of inhibitory checkpoints on CD8+ T cells in tumors. J Exp Med 2015;212:139–48.
13. Zheng H, Guo X, Tian Q, Li H, Zhu Y. Distinct role of Tim-3 in systemic lupus erythematosus and clear cell renal cell carcinoma. Int J Clin Exp Med 2015;8:7029–38.
14. Badoual C, Hans S, Merillon N, Van Ryswick C, Ravel P, Benhamouda N, et al. PD-1-expressing tumor-infiltrating T cells are a favorable prognostic biomarker in HPV-associated head and neck cancer. Cancer Res 2013;73:128–38.
15. R Core Team. R : a language and environment for statistical computing. Vienna, Austria: R Foundation for Statistical Computing; 2015.
16. Blackburn SD, Shin H, Freeman GJ, Wherry EJ. Selective expansion of a subset of exhausted CD8 T cells by alphaPD-L1 blockade. Proc Natl Acad Sci U S A 2008;105:15016–21.
17. Carreras J, Lopez-Guillermo A, Roncador G, Villamor N, Colomo L, Martinez A, et al. High numbers of tumor-infiltrating programmed cell death 1-positive regulatory lymphocytes are associated with improved overall survival in follicular lymphoma. J Clin Oncol 2009;27:1470–6.
18. Muenst S, Soysal SD, Gao F, Obermann EC, Oertli D, Gillanders WE. The presence of programmed death 1 (PD-1)-positive tumor-infiltrating lymphocytes is associated with poor prognosis in human breast cancer. Breast Cancer Res Treat 2013;139:667–76.
19. Mlecnik B, Tosolini M, Charoentong P, Kirilovsky A, Bindea G, Berger A, et al. Biomolecular network reconstruction identifies T-cell homing factors associated with survival in colorectal cancer. Gastroenterology 2010;138:1429–40.
20. Odorizzi PM, Pauken KE, Paley MA, Sharpe A, Wherry EJ. Genetic absence of PD-1 promotes accumulation of terminally differentiated exhausted CD8+ T cells. J Exp Med 2015;212:1125–37.
21. Yang ZZ, Grote DM, Ziesmer SC, Niki T, Hirashima M, Novak AJ, et al. IL-12 upregulates TIM-3 expression and induces T cell exhaustion in patients with follicular B cell non-Hodgkin lymphoma. J Clin Invest 2012;122:1271–82.
22. Severson JJ, Serracino HS, Mateescu V, Raeburn CD, McIntyre RCJr, Sams SB, et al. PD-1+Tim-3+ CD8+ T lymphocytes display varied degrees of functional exhaustion in patients with regionally metastatic differentiated thyroid cancer. Cancer Immunol Res 2015;3:620–30.
23. Takamura S, Tsuji-Kawahara S, Yagita H, Akiba H, Sakamoto M, Chikaishi T, et al. Premature terminal exhaustion of Friend virus-specific effector CD8+ T cells by rapid induction of multiple inhibitory receptors. J Immunol 2010;184:4696–707.
24. Jin HT, Anderson AC, Tan WG, West EE, Ha SJ, Araki K, et al. Cooperation of Tim-3 and PD-1 in CD8 T-cell exhaustion during chronic viral infection. Proc Natl Acad Sci U S A 2010;107:14733–8.
25. Cai C, Xu YF, Wu ZJ, Dong Q, Li MY, Olson JC, et al. Tim-3 expression represents dysfunctional tumor infiltrating T cells in renal cell carcinoma. World J Urol 2016;34:561–7.
26. Terawaki S, Chikuma S, Shibayama S, Hayashi T, Yoshida T, Okazaki T, et al. IFN-α directly promotes programmed cell death-1 transcription and limits the duration of T cell-mediated immunity. J Immunol 2011;186:2772–9.
27. Zhu C, Sakuishi K, Xiao S, Sun Z, Zaghouani S, Gu G, et al. An IL-27/NFIL3 signalling axis drives Tim-3 and IL-10 expression and T-cell dysfunction. Nat Commun 2015;6:6072.
28. Dannenmann SR, Thielicke J, Stockli M, Matter C, von Boehmer L, Cecconi V, et al. Tumor-associated macrophages subvert T-cell function and correlate with reduced survival in clear cell renal cell carcinoma. Oncoimmunology 2013;2:e23562.
29. Tang D, Lotze MT. Tumor immunity times out: TIM-3 and HMGB1. Nat Immunol 2012;13:808–10.
30. Chiba S, Baghdadi M, Akiba H, Yoshiyama H, Kinoshita I, Dosaka-Akita H, et al. Tumor-infiltrating DCs suppress nucleic acid-mediated innate immune responses through interactions between the receptor TIM-3 and the alarmin HMGB1. Nat Immunol 2012;13:832–42.
31. Komohara Y, Morita T, Annan DA, Horlad H, Ohnishi K, Yamada S, et al. The coordinated actions of TIM-3 on cancer and myeloid cells in the regulation of tumorigenicity and clinical prognosis in clear cell renal cell carcinomas. Cancer Immunol Res 2015;3:999–1007.
32. Sakuishi K, Ngiow SF, Sullivan JM, Teng MW, Kuchroo VK, Smyth MJ, et al. TIM3+FOXP3+ regulatory T cells are tissue-specific promoters of T-cell dysfunction in cancer. Oncoimmunology 2013;2:e23849.
33. van Esch EM, van Poelgeest MI, Kouwenberg S, Osse EM, Trimbos JB, Fleuren GJ, et al. Expression of coinhibitory receptors on T cells in the microenvironment of usual vulvar intraepithelial neoplasia is related to proinflammatory effector T cells and an increased recurrence-free survival. Int J Cancer 2015;136:E95–106.
34. Matsuzaki J, Gnjatic S, Mhawech-Fauceglia P, Beck A, Miller A, Tsuji T, et al. Tumor-infiltrating NY-ESO-1-specific CD8+ T cells are negatively regulated by LAG-3 and PD-1 in human ovarian cancer. Proc Natl Acad Sci U S A 2010;107:7875–80.
35. Nakano O, Sato M, Naito Y, Suzuki K, Orikasa S, Aizawa M, et al. Proliferative activity of intratumoral CD8(+) T-lymphocytes as a prognostic factor in human renal cell carcinoma: clinicopathologic demonstration of antitumor immunity. Cancer Res 2001;61:5132–6.
36. Schalper KA, Brown J, Carvajal-Hausdorf D, McLaughlin J, Velcheti V, Syrigos KN, et al. Objective measurement and clinical significance of TILs in non-small cell lung cancer. J Natl Cancer Inst 2015;107;pii:dju435.